PERGAMON

International Journal of Solids and Structures 38 (2001) 5007–5018

INTERNATIONAL JOURNAL OF SOLIDS and STRUCTURES

www.elsevier.com/locate/ijsolstr

Stress analysis for a Zener–Stroh crack interacting with a coated inclusion

Z.M. Xiao *, B.J. Chen

School of Mechanical and Production Engineering, Nanyang Technological University, Nanyang Avenue, Singapore 639798, Singapore

Received 12 May 2000

Abstract

A microcrack can be initiated by coalescing dislocations piled up near an inhomogeneity. This mechanism was firstly proposed by Zener and later analyzed by Stroh. The microcrack thus is called a Zener–Stroh crack, a counterpart of the well-known Griffith crack in linear elastic fracture mechanics. In the current study we consider a Zener–Stroh crack initiated near a coated circular fiber in a solid material. The interaction between the crack and the coated inclusion (fiber) for both Mode I and II displacement loading is investigated using the solution of an edge dislocation interacting with a coated fiber derived by Xiao and Chen [International Journal of Solids and Structure, in press] as the Green's function. The problem is formulated as a set of singular integral equations and is solved numerically by Erdogan–Gupta method. The influence of several parameters, such as the distance between the crack and the inclusion, the material constants combination of the fiber, the coating layer and the matrix, on the stress intensity factors of the crack is analyzed. Several numerical examples are given and the results obtained are discussed in detail.

Keywords: Crack; Inclusion; Interaction; Stress intensity factor; Dislocation

1. Introduction

1.1. Crack–inclusion interaction

The increasing application of composite materials in engineering structures has made investigations on crack–inclusion interactions popular. The load carrying capacity of composite materials may be reduced significantly by the defects such as microcracks contained inside the materials. As the fracture behavior of a crack in a composite is greatly influenced by the nearby reinforcing phase (such as fibers or hard particles), the study on crack–inclusion interaction becomes crucial in understanding the fracture toughness of a composite material. A lot of research work dealing with the topic can be found in open literature. To name a few, the interaction between a crack and a circular inclusion in a sheet under tension was studied by

* Corresponding author. Tel.: +65-790-4726; fax: +65-791-1859.
E-mail address: mzxiao@ntu.edu.sg (Z.M. Xiao).

0020-7683/01/$ - see front matter
PII: S0020-7683(00)00335-8

Tamate (1968). An elastic circular inclusion interacting with two symmetrically placed collinear cracks was investigated by Hsu and Shivakumar (1976). Sendeckyj (1974) studied the problem of a crack located between two rigid inclusion. The investigation for a crack near an elliptic inclusion was carried in terms of body force method by Nisitani et al. (1996).

It is noted that all the above mentioned research involves two dissimilar material phases only, i.e., the inclusion phase and the matrix phase. In some advanced fiber-reinforced composite materials, in order to increase the interfacial bonding strength between the fiber and the matrix, a coating layer on fiber is introduced. It is well known that the considerable toughness in composites with brittle, but strong reinforcing fibers can be achieved by controlling debonding of the fibers from the matrix to prevent premature fracture of the composite. Thus coating on fibers is often employed to improve the mechanical strength of composite materials. The coating effect on the stress field was first studied by Mikata and Taya (1985a,b) for the problem of a coated fiber embedded in infinitely extended matrix. However, to the best knowledge of the authors, so far no research work on the interaction between a crack and a coated inclusion has been published. Three dissimilar material phases (the matrix, the fiber and the coating layer) are involved in such an elastic problem. The main objective of the current paper is to investigate the interaction between a crack and a coated fiber.

1.2. Zener–Stroh crack

It was Zener (1948) who first proposed that a pileup of edge dislocations that were stopped at an obstacle, such as a grain boundary, could coalesce into a crack nucleus. Stroh (1954) made a detailed calculation to find how many dislocations are needed to form a microcrack. His first estimation was that 10^3 dislocations are necessary for work-hardened copper. Later on he found a number of the order of 10^2 is required if a stack of piled-up dislocations on parallel slip planes exist. As sketched in Fig. 1, investigation carried out by Kikuchi et al. (1981) shows that, when a particle in a solid matrix is stressed, concentrated stress fields exist near the ends of the particle, slip is thus nucleated in these regions. Dislocations of one sign move away from the region, leaving stationary dislocations of the opposite sign behind to form a crack near the particle. This is the experimental background for the current study.

As a Zener–Stroh crack is formed by a dislocation pileup, therefore it is a net dislocation loaded crack. Due to the displacement loading mechanism, the total sum of the Burgers vectors of the dislocations b_T within a Zener–Stroh crack does not equal zero. The crack tip where the dislocation enters the Zener–Stroh crack is called the blunt tip, while the other tip is called the sharp tip. The propagation of a Zener–Stroh crack is always along the sharp crack tip. The stress, displacement, dislocation density and stress intensity factor were compared between Zener–Stroh crack and Griffith crack by Weertman (1986).

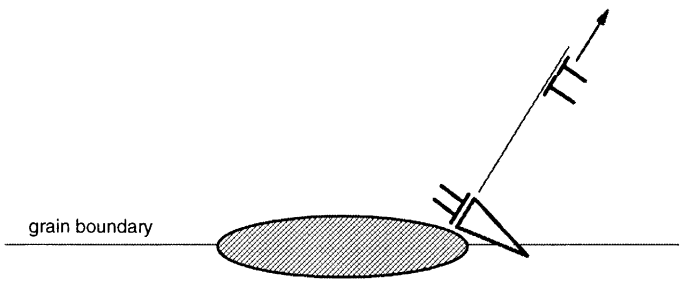

Fig. 1. A Zener–Stroh crack initiated near an inclusion.

2. Problem formulation

The physical problem to be solved is shown in Fig. 2, where medium number 1 (the fiber), with elastic properties κ_1 and μ_1, occupies the inner circular region $r \leqslant a$; medium number 2 (the coating layer), with elastic properties κ_2 and μ_2, occupies the intermediate annular region $a \leqslant r \leqslant b$; and medium number 3 (the infinitely extended matrix), with elastic properties κ_3 and μ_3, occupies the outer infinite region $r \geqslant b$. A Zener–Stroh crack is initiated near the coated circular inclusion (the coated fiber), and is located in the radial direction within the matrix phase. Since too many parameters are involved in the current engineering problem, we assume no external mechanical loading is applied on the body. While we do have the displacement loading, i.e., the net dislocations inside the Zener–Stroh crack. It should be noted that the problem can be solved without extra difficulty even with external mechanical loading. As the problem is linear elastic, what one needs to do is to superpose the mechanical load to the displacement load.

The boundary conditions for the current problem are:

In the far field,

$$\sigma_{xy} = 0, \qquad \sigma_{yy} = 0. \tag{1}$$

At the interface,

$$[\sigma_{rr}] = 0, \qquad [\sigma_{r\theta}] = 0. \tag{2}$$

Along the crack surface,

$$\sigma_{xy} = 0, \qquad \sigma_{yy} = 0, \quad t_1 \leqslant x \leqslant t_2, \tag{3}$$

where $[f]$ denotes the jump of the function f. In order to solve the problem, the equivalence between a crack and a continuously distribution of dislocations is employed. Setting $B_x(x)$ and $B_y(x)$ be the gliding and climbing dislocation densities in the crack site $t_1 \leqslant x \leqslant t_2$, and using the stress analysis results of an edge dislocation near a coated fiber derived by Xiao and Chen (2000) as the Green's functions, the traction at $(x, 0)$ due to these dislocation distributions is

$$\sigma_{yy}(x,0) = -\frac{2\mu_3}{\kappa_3+1}\frac{1}{\pi}\left[\int_{t_1}^{t_2}\frac{B_y(\xi)}{\xi - x}\mathrm{d}\xi + \int_{t_1}^{t_2} k_1(x,\xi)B_y(\xi)\mathrm{d}\xi\right], \tag{4a}$$

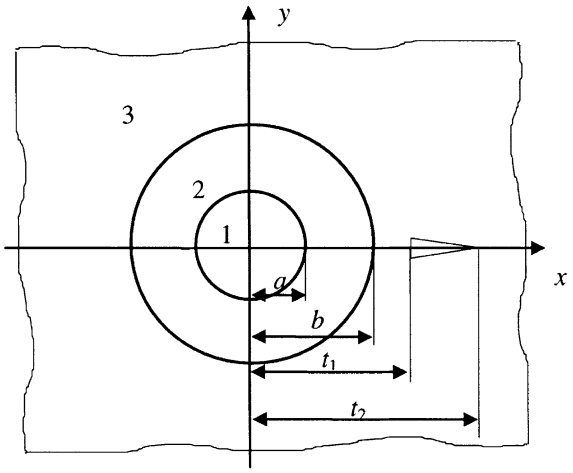

Fig. 2. The physical model of the current problem.

$$\sigma_{xy}(x,0) = -\frac{2\mu_3}{\kappa_3+1}\frac{1}{\pi}\left[\int_{t_1}^{t_2}\frac{B_x(\xi)}{\xi-x}\mathrm{d}\xi + \int_{t_1}^{t_2}k_2(x,\xi)B_x(\xi)\mathrm{d}\xi\right]. \tag{4b}$$

With the aid of the above equations, the traction free conditions on the upper and lower crack surface (the boundary condition (3)) are written in terms of B_x, B_y as

$$\frac{1}{\pi}\int_{t_1}^{t_2}\frac{B_y(\xi)}{\xi-x}\mathrm{d}\xi + \int_{t_1}^{t_2}\frac{1}{\pi}k_1(x,\xi)B_y(\xi)\mathrm{d}\xi = 0, \quad t_1 \leqslant x \leqslant t_2, \tag{5a}$$

$$\frac{1}{\pi}\int_{t_1}^{t_2}\frac{B_x(\xi)}{\xi-x}\mathrm{d}\xi + \int_{t_1}^{t_2}\frac{1}{\pi}k_2(x,\xi)B_x(\xi)\mathrm{d}\xi = 0, \quad t_1 \leqslant x \leqslant t_2. \tag{5b}$$

Moreover, the dislocation densities $B_x(x)$ and $B_y(x)$ must satisfy

$$\int_{t_1}^{t_2}B_y(\xi)\mathrm{d}\xi = b_y^{\mathrm{T}}, \tag{6a}$$

$$\int_{t_1}^{t_2}B_x(\xi)\mathrm{d}\xi = b_x^{\mathrm{T}}, \tag{6b}$$

where b_x^{T} and b_y^{T} are the total sums of Burgers vectors of the net dislocations inside the Zener–Stroh crack. The two integral kernels $k_1(x,\xi)$, $k_2(x,\xi)$ in Eqs. (5a) and (5b) have the expressions

$$\begin{aligned} k_1(x,\xi) = {} & \frac{C+D}{2(x-b^2/\xi)} + C\frac{\xi^2-b^2}{\xi^3}\frac{b^2}{(x-b^2/\xi)^2}\left(\frac{\xi^2}{b^2}-\frac{\xi^2-b^2)}{x\xi-b^2}\right) - \frac{C+D}{2x} - \frac{1-CD}{2(1-C)}a_0\frac{b}{x^2} - \frac{1}{2\xi} \\ & \times\frac{b^2}{x^2}\left(2C\frac{\xi^2}{b^2}-C-1\right) - C\frac{b^2}{x^3} - \frac{(1-CD)}{(1-D)b}\sum_{n=1}^{\infty}a_{-n}\left(\frac{b}{x}\right)^n + \frac{(1-CD)}{2(1-D)b}\left\{\sum_{n=1}^{\infty}na_{-n}\left(\frac{b}{x}\right)^n\right. \\ & \left. -\sum_{n=1}^{\infty}(n+1)a_{-n}\left(\frac{b}{x}\right)^{n+2}\right\} - \frac{(1-CD)}{2(1-C)b}\sum_{n=1}^{\infty}a_n\left(\frac{b}{x}\right)^{n+2}, \end{aligned} \tag{7a}$$

and

$$\begin{aligned} k_2(x,\xi) = {} & \frac{C+D}{2(x-b^2/\xi)} + C\frac{b^2}{(x-b^2/\xi)^2}\left(\frac{x-\xi}{\xi^2}\frac{\xi^2-b^2}{x\xi-b^2}\right) - \frac{C+D}{2x} - \frac{1-C}{2\xi}\frac{b^2}{x^2} + C\frac{b^2}{x^3} \\ & + \frac{1-CD}{2(1-C)}a_0'\frac{b}{x^2} + \frac{(1-CD)}{2(1-D)b}\sum_{n=1}^{\infty}na_{-n}'\left(\frac{b}{x}\right)^n - \frac{(1-CD)}{2(1-D)b}\sum_{n=1}^{\infty}(n+1)a_{-n}'\left(\frac{b}{x}\right)^{n+2} \\ & + \frac{(1-CD)}{2(1-C)b}\sum_{n=1}^{\infty}a_n'\left(\frac{b}{x}\right)^{n+2}, \end{aligned} \tag{7b}$$

where the detailed expressions of the coefficients a_n and a_n' can be found in Xiao and Chen (2000), and

$$C = \frac{\mu_3-\mu_2}{\mu_2\kappa_3+\mu_3}, \qquad D = \frac{\mu_3\kappa_2-\mu_2\kappa_3}{\mu_3\kappa_2+\mu_2}. \tag{8}$$

Eqs. (5a) and (5b) are the standard singular integral equations with Cauchy type regular kernels. Once the dislocation densities B_x, B_y are solved from Eqs. (5a), (5b) and (6a), (6b) the stress fields in the matrix phase can be obtained from Eqs. (4a) and (4b). Since the whole crack is located in the pure matrix material, the singularities on the both crack tips should be inverse square root. As a result, the two dislocation density functions must have inverse square root singular behaviors on the both crack tips. Let

$$B_x(x) = w(x)F_x(x), \qquad B_y(x) = w(x)F_y(x), \tag{9}$$

where $F_x(x)$ and $F_y(x)$ are non-singular smooth functions in $t_1 \leqslant x \leqslant t_2$, and

$$w(x) = (x - t_1)^{-(1/2)}(t_2 - x)^{-(1/2)} \tag{10}$$

is called the fundamental function of the integral equations (Erdogan and Gupta, 1972).

3. Numerical procedures

To shift the integral interval from (t_1, t_2) to $(-1, 1)$, we take

$$x = \frac{t_2 - t_1}{2}t + \frac{t_2 + t_1}{2}, \qquad \xi = \frac{t_2 - t_1}{2}s + \frac{t_2 + t_1}{2}. \tag{11}$$

Eqs. (5a) and (5b) are rewritten in terms of s, t as:

$$\frac{1}{\pi}\int_{-1}^{1}\frac{B_y(s)}{s - t}\mathrm{d}s + \frac{1}{\pi}\int_{-1}^{1}k_{11}(t, s)B_y(s)\mathrm{d}s = 0, \quad -1 \leqslant s, \quad t \leqslant 1, \tag{12a}$$

$$\frac{1}{\pi}\int_{-1}^{1}\frac{B_x(s)}{s - t}\mathrm{d}s + \frac{1}{\pi}\int_{-1}^{1}k_{22}(t, s)B_x(s)\mathrm{d}s = 0, \quad -1 \leqslant s, \quad t \leqslant 1, \tag{12b}$$

where

$$k_{11}(t, s) = \frac{t_2 - t_1}{2}k_1\Big(\frac{t_2 - t_1}{2}t + \frac{t_2 + t_1}{2}, \frac{t_2 - t_1}{2}s + \frac{t_2 + t_1}{2}\Big), \tag{13a}$$

$$k_{22}(t, s) = \frac{t_2 - t_1}{2}k_2\Big(\frac{t_2 - t_1}{2}t + \frac{t_2 + t_1}{2}, \frac{t_2 - t_1}{2}s + \frac{t_2 + t_1}{2}\Big), \tag{13b}$$

and Eqs. (6a) and (6b) are similarly rewritten as

$$\int_{-1}^{1}B_y(s)\mathrm{d}s = \frac{2b_y^{\mathrm{T}}}{t_2 - t_1}, \tag{14a}$$

$$\int_{-1}^{1}B_x(s)\mathrm{d}s = \frac{2b_x^{\mathrm{T}}}{t_2 - t_1}. \tag{14b}$$

Following the method developed by Erdogan and Gupta (1972), the discretized forms of Eqs. (12a), (12b) and (14a), (14b) are obtained as

$$\sum_{k=1}^{n}\frac{1}{n}F_y(s_k)\left[\frac{1}{s_k - u_r} + k_{11}(u_r, s_k)\right] = 0, \tag{15a}$$

$$\sum_{k=1}^{n}\frac{1}{n}F_x(s_k)\left[\frac{1}{s_k - u_r} + k_{22}(u_r, s_k)\right] = 0, \tag{15b}$$

$$\sum_{k=1}^{n}\frac{1}{n}F_y(s_k) = \frac{b_y^{\mathrm{T}}}{\pi}\frac{2}{t_2 - t_1}, \tag{15c}$$

$$\sum_{k=1}^{n}\frac{1}{n}F_x(s_k) = \frac{b_x^{\mathrm{T}}}{\pi}\frac{2}{t_2 - t_1}, \tag{15d}$$

in which

$$s_k = \cos\frac{\pi}{2n}(2k-1), \qquad u_r = \cos\frac{\pi r}{n}, \quad k = 1,\ldots,n, \quad r = 1,\ldots,n-1. \tag{15e}$$

Eqs. (15a) and (15c) provide a system of n linear algebraic equations to determine the values of $F_y(s_1),\ldots,F_y(s_n)$, and Eqs. (15b) and (15d) provide a system of n linear algebraic equations to determine the values of $F_x(s_1),\ldots,F_x(s_n)$.

With the numerical solution of the dislocation density functions, the Modes I and II stress intensity factors (SIFs) on the left (the blunt) and right (the sharp) crack tips are then given by (Weertman, 1996)

$$K_{\mathrm{I}}^{\mathrm{L}} = -\lim_{\xi\to t_1}\frac{2\mu_3\sqrt{2\pi}}{1+\kappa_3}\sqrt{\xi-t_1}B_y(\xi) = -\frac{2\mu_3}{(1+\kappa_3)}\frac{b_y^{\mathrm{T}}}{\sqrt{\pi(t_2-t_1)/2}}F_y(-1), \tag{16a}$$

$$K_{\mathrm{II}}^{\mathrm{L}} = -\lim_{\xi\to t_1}\frac{2\mu_3\sqrt{2\pi}}{1+\kappa_3}\sqrt{\xi-t_1}B_x(\xi) = -\frac{2\mu_3}{(1+\kappa_3)}\frac{b_x^{\mathrm{T}}}{\sqrt{\pi(t_2-t_1)/2}}F_x(-1), \tag{16b}$$

$$K_{\mathrm{I}}^{\mathrm{R}} = \lim_{\xi\to t_2}\frac{2\mu_3\sqrt{2\pi}}{1+\kappa_3}\sqrt{t_2-\xi}B_y(\xi) = \frac{2\mu_3}{(1+\kappa_3)}\frac{b_y^{\mathrm{T}}}{\sqrt{\pi(t_2-t_1)/2}}F_y(1), \tag{16c}$$

$$K_{\mathrm{I}}^{\mathrm{R}} = \lim_{\xi\to t_2}\frac{2\mu_3\sqrt{2\pi}}{1+\kappa_3}\sqrt{t_2-\xi}B_x(\xi) = \frac{2\mu_3}{(1+\kappa_3)}\frac{b_x^{\mathrm{T}}}{\sqrt{\pi(t_2-t_1)/2}}F_x(1), \tag{16d}$$

where the superscripts L and R represent the left and right crack tips, respectively.

4. Numerical results and discussion

For the numerical examples given in this section, to emphasize the influence of the coated fiber on the crack, the SIFs of the crack are normalized by

$$K_{\mathrm{I}}^0 = \frac{2\mu_3 b_y^{\mathrm{T}}}{(1+\kappa_3)\sqrt{\pi(t_2-t_1)/2}}, \qquad K_{\mathrm{II}}^0 = \frac{2\mu_3 b_x^{\mathrm{T}}}{(1+\kappa_3)\sqrt{\pi(t_2-t_1)/2}}, \tag{17}$$

which are the respective Modes I and II SIFs of a Zener–Stroh crack in a homogeneous material (without the inclusion) but with the same crack size and same displacement loads as the current problem. In our calculations, it is found that the SIFs at the blunt tip (the left crack tip) are always negative. These results are consistent to our discussion in the introduction, i.e., the propagation of a Zener–Stroh crack is always along the sharp crack tip.

4.1. Influence of the shear modulus of the fiber on the behavior of the crack

The variations of normalized Modes I and II SIFs with the shear modulus ratio μ_1/μ_3 are depicted in Figs. 3–6, for the both crack tips and different coating layer thickness $b/a = 1.05, 1.2, 1.5$, respectively. The other parameters are taken as $t_1 = 1.05b$, $t_2 = 1.35b$ and $\mu_2/\mu_3 = 2.33$, $\nu_1 = 0.3$, $\nu_2 = 0.28$, $\nu_3 = 0.3$. This materials constants combination is based on a typical TiAl matrix reinforced by SiC fiber with W coating layer (Hahn, 1993). It is shown that the influence of the elastic property of the fibers becomes less sensitive when b/a increases. This result is reasonable. As the coating layer is getting thicker, the effect of the fiber is shielded by the coating layer. In the figures, all the curves intersects at the point where $\mu_1 = \mu_2$. This is because at this point, the current problem is reduced to the two-phase case (without the coating layer). One

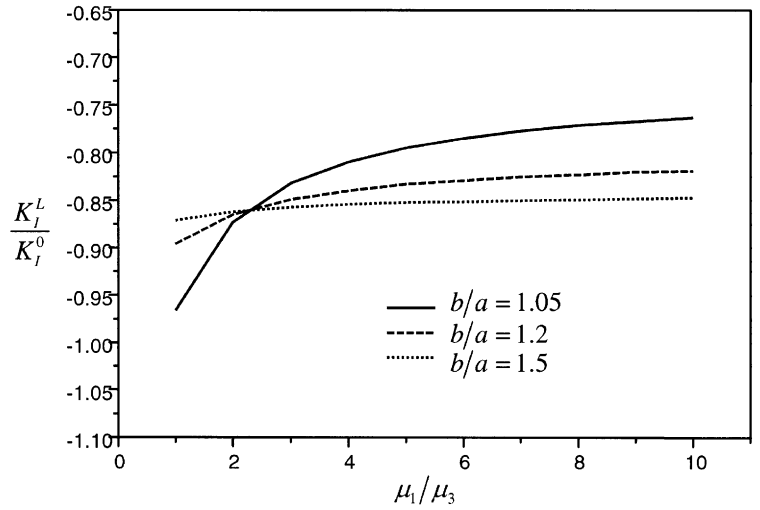

Fig. 3. Normalized $K_{\mathrm{I}}^{\mathrm{L}}$ versus μ_1/μ_3 for $\mu_2/\mu_3 = 2.33$, $t_1 = 1.05b$, $t_2 = 1.35b$.

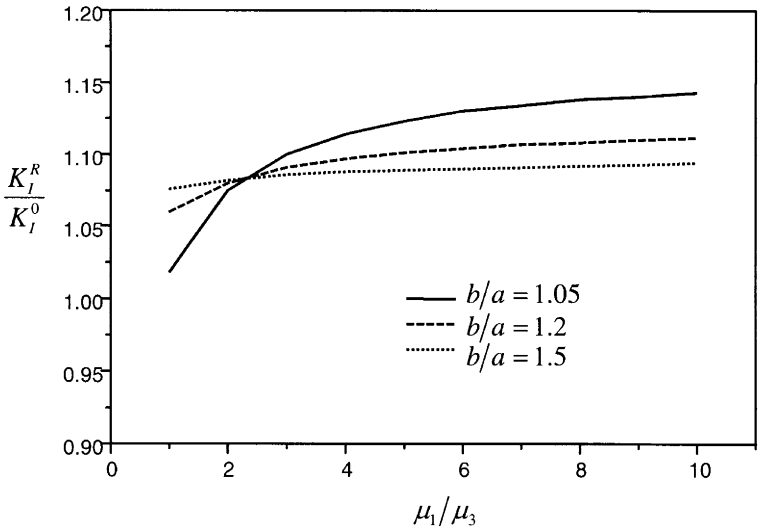

Fig. 4. Normalized $K_{\mathrm{I}}^{\mathrm{R}}$ versus μ_1/μ_3 for $\mu_2/\mu_3 = 2.33$, $t_1 = 1.05b$, $t_2 = 1.35b$.

interesting result is that for the right crack tip (the sharp tip), the values of normalized SIF are greater than 1. This result indicates that a "hard" inclusion makes a displacement loaded Zener–Stroh easier to propagate, which is totally opposite to a Griffith crack case: a "hard" inclusion retards the propagation of a stress loaded Griffith crack. It is worth to note that the Zener–Stroh mechanism dominates the crack behavior only when the crack is just initiated at its micro level. As the crack size increases, the Griffith mechanism will dominate the propagation of the crack.

Since the SIFs at the left crack tip (the blunt tip) are always negative, the crack will never propagate from this tip. In the following calculations, only the results for the right crack tip are plotted and discussed.

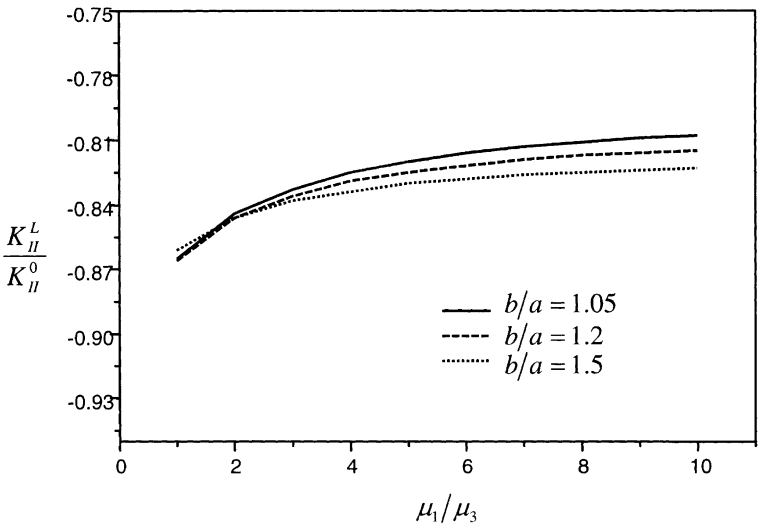

Fig. 5. Normalized $K_{\mathrm{II}}^{\mathrm{L}}$ versus μ_1/μ_3 for $\mu_2/\mu_3 = 2.33$, $t_1 = 1.05b$, $t_2 = 1.35b$.

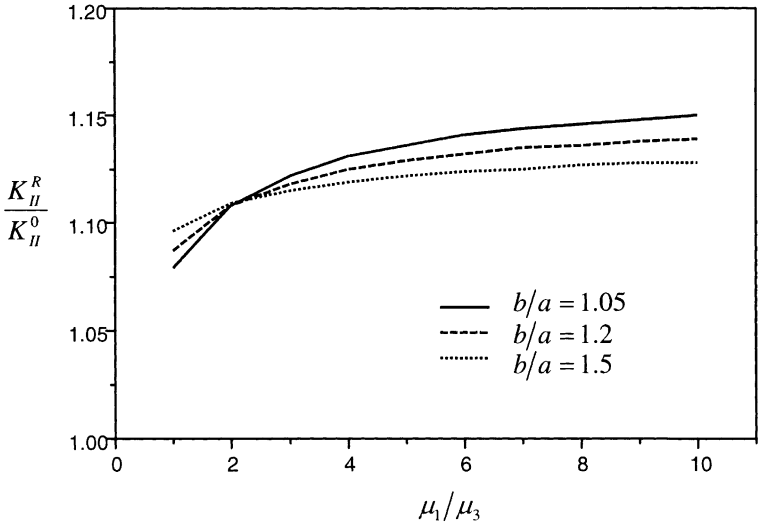

Fig. 6. Normalized $K_{\mathrm{II}}^{\mathrm{R}}$ versus μ_1/μ_3 for $\mu_2/\mu_3 = 2.33$, $t_1 = 1.05b$, $t_2 = 1.35b$.

4.2. Influence of the shear modulus of the coating layer on the behavior of the crack

The normalized Modes I and II SIFs at the right crack tip versus μ_2/μ_3 are plotted in Figs. 7 and 8, respectively, with the other parameters are taken as $t_1 = 1.05b$, $t_2 = 1.35b$, $b/a = 1.1$, $\mu_1/\mu_3 = 2.44$ and $v_1 = v_2 = v_3 = 0.3$. The material property combination is based on coated SiC fiber in TiAl matrix (Hahn, 1993). The solutions of the two-phase case (without the coating layer) for $\mu_1/\mu_3 = 2.44$ are also shown in the figures. It is found that the SIFs increase with the increasing value of μ_2/μ_3. As discussed in the previous sub-section, this result is again opposite to the case of a stress loaded Griffith crack. Also similar to the case given in Section 4.1, the two curves in the figures intersect at the point where $\mu_1 = \mu_2$.

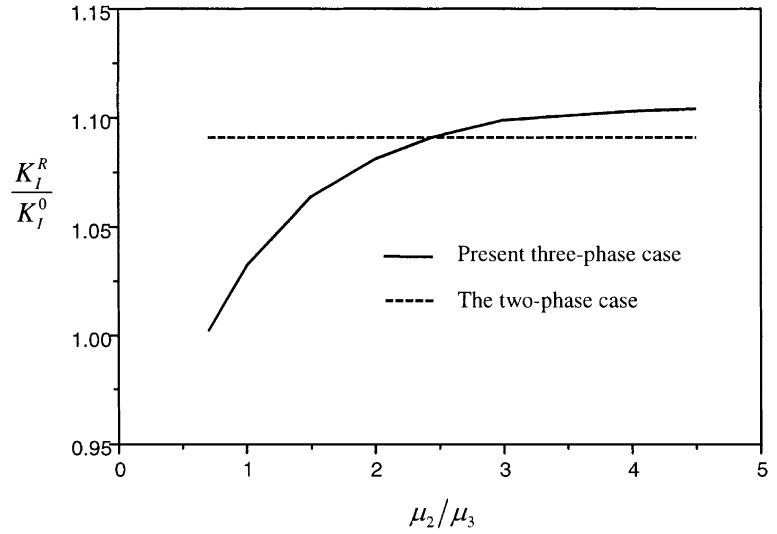

Fig. 7. Normalized $K_{\mathrm{I}}^{\mathrm{R}}$ versus μ_2/μ_3 for $\mu_1/\mu_3 = 2.44$, $b/a = 1.1$, $t_1 = 1.05b$, $t_2 = 1.35b$.

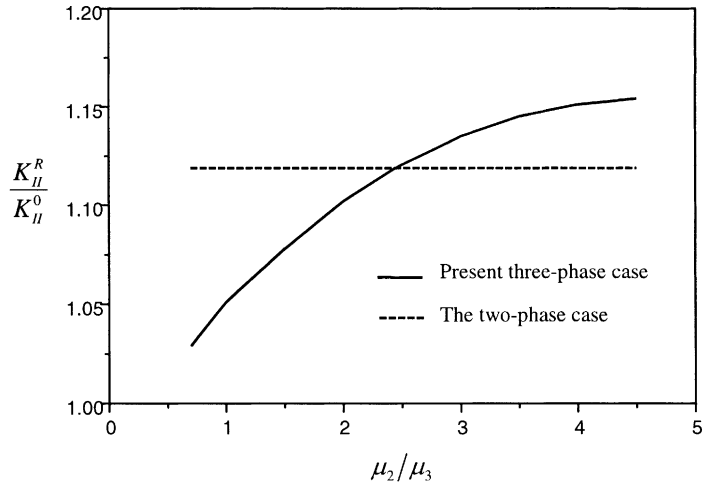

Fig. 8. Normalized $K_{\mathrm{II}}^{\mathrm{R}}$ versus μ_2/μ_3 for $\mu_1/\mu_3 = 2.44$, $b/a = 1.1$, $t_1 = 1.05b$, $t_2 = 1.35b$.

4.3. Influence of the coating thickness on the behavior of the crack

The normalized SIFs for the right crack tip versus the coating thickness b/a are depicted in Figs. 9 and 10, respectively. The other parameters are taken as: $\mu_1/\mu_3 = 2.44$, $\mu_2/\mu_3 = 1.86$, $t_1 = 1.05b$, $t_2 = 1.35b$ and $v_1 = v_2 = v_3 = 0.3$. The material constants are based on SiC fiber coated by Mo in TiAl matrix (Hahn, 1993). For comparison purpose, the result for the two-phase case $\mu_1/\mu_3 = 2.44$ is also displayed. It is found that the SIFs decrease with the increasing of the coating thickness. This is because the coating material is "harder" than the matrix in this case.

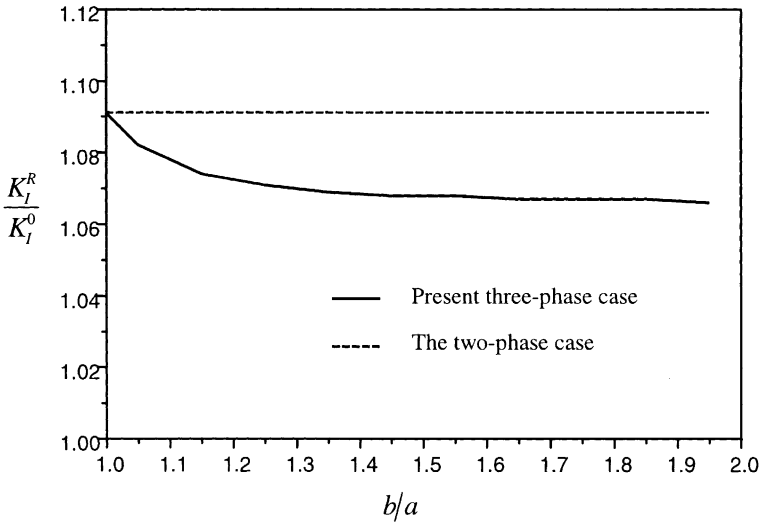

Fig. 9. Variation of normalized $K_{\mathrm{I}}^{\mathrm{R}}$ with coating thickness b/a for $\mu_1/\mu_3 = 2.44$, $\mu_2/\mu_3 = 1.86$, $t_1 = 1.05b$, $t_2 = 1.35b$.

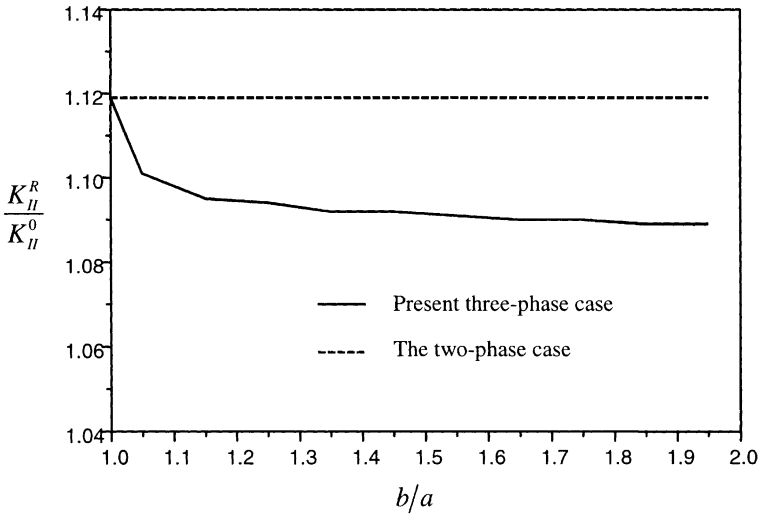

Fig. 10. Variation of normalized $K_{\mathrm{II}}^{\mathrm{R}}$ with coating thickness b/a for $\mu_1/\mu_3 = 2.44$, $\mu_2/\mu_3 = 1.86$, $t_1 = 1.05b$, $t_2 = 1.35b$.

4.4. Influence of the distance between the crack and the inclusion on the behavior of the crack

The normalized SIFs at the right crack tip against $(t_2 + t_1)/2b$ are plotted in Figs. 11 and 12, respectively, where the length of the crack is fixed at $t_2 - t_1 = 0.5b$. The other parameters are taken as $\mu_1/\mu_3 = 5.43$, $\mu_2/\mu_3 = 3.33$ and $\nu_1 = \nu_2 = \nu_3 = 0.25$, which are based on SnO_2 coated alumina PRD-166 in glass matrix (Chaula, 1993). The value of the SIFs decreases with the increasing distance between the crack and the inclusion. This result is consistent with conventional crack–inclusion interaction problems. As the distance increases, the influence of the inclusion to the crack will be weakened.

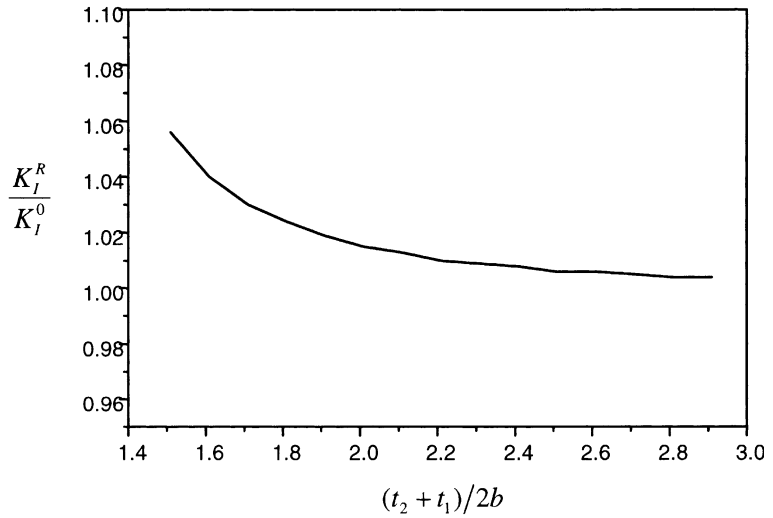

Fig. 11. Normalized $K_{\mathrm{I}}^{\mathrm{R}}$ versus distance for $\mu_1/\mu_3 = 5.43$, $\mu_2/\mu_3 = 3.33$, $b/a = 1.1$, $t_2 - t_1 = 0.5b$.

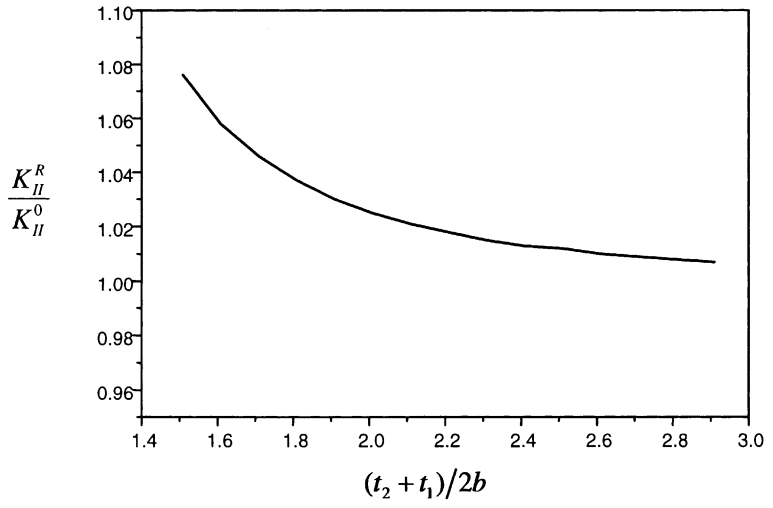

Fig. 12. Normalized $K_{\mathrm{II}}^{\mathrm{R}}$ versus distance for $\mu_1/\mu_3 = 5.43$, $\mu_2/\mu_3 = 3.33$, $b/a = 1.1$, $t_2 - t_1 = 0.5b$.

5. Conclusions

The interaction between a Zener–Stroh crack and a coated inclusion is investigated. The SIFs for the both crack tips are analyzed. It is found that the SIFs at the blunt crack tip is always negative, which indicates the propagation of a Zener–Stroh crack is always along its sharp tip. Also we find that a near-by "hard" inclusion amplifies the SIFs of a displacement loaded Zener–Stroh crack, i.e., a "hard" inclusion makes the crack easier to propagate. When the thickness of coating layer increases, the influence of the fiber to the crack is shielded by the coating layer, and the result obtained is gradually approaching to the two-phase case.

References

Chaula, K.K., 1993. Interface mechanics and toughness. Ceramic Matrix Composites 291–339.

Erdogan, F., Gupta, G.D., 1972. On the numerical solution of singular integral equations. Quarterly of Applied Mathematics 30, 525–534.

Hahn, T.A., 1993. Thermal stress relaxation due to plastic flow in the fiber coating of a continuous fiber reinforced composite. Journal of Composite Materials 27, 1545–1577.

Hsu, Y.C., Shivakumar, V., 1976. Interaction between an elastic circular inclusion and two symmetrically placed collinear cracks. International Journal of Fracture Mechanics 12, 619–630.

Kikuchi, M., Shiozawa, K., Weertman, J., 1981. Void nucleation in astrology. Acta Mechanics 29, 1747–1758.

Mikata, Y., Taya, M., 1985a. Stress field in and around a coated short fiber in infinite matrix subjected to uniaxial and biaxial loadings. ASME Journal of Applied Mechanics 52, 19–24.

Mikata, Y., Taya, M., 1985b. Stress field in a coated continuous fiber composite subjected to thermal-mechanical loadings. Journal of Composite Materials 19, 554–578.

Nisitani, H., Chen, D.H., Saimoto, A., 1996. Interaction between an elliptic inclusion and a crack. Proceedings of the International Conference on Computer-Aided Assessment and Control, Computational Mechanics Inc., MA, USA, vol. 4, 1996, pp. 325–332.

Sendeckyj, G.P., 1974. Interaction of cracks with rigid inclusions in longitudinal shear deformation. International Journal of Fracture Mechanics 10, 45–52.

Stroh, A.N., 1954. The formation of cracks as a result of plastic flow, I. Proceedings of Royal Society of London A 223, 404–414.

Tamate, O., 1968. The effect of a circular inclusion on the stresses around a line crack in a sheet under tension. International Journal of Fracture Mechanics 4, 257–265.

Weertman, J., 1986. Zener–Stroh crack, Zener–Hollomon parameter, and other topics. Journal of Applied Physics 60, 1877–1887.

Weertman, J., 1996. Dislocation Based Fracture Mechanics. World Scientific, Singapore.

Xiao, Z.M., Chen, B.J., 2000. An edge dislocation interacting with a coated fiber. International Journal of Solids and Structures, in press.

Zener, C., 1948. The micro-mechanism of fracture. Fracturing of Metals, Cleveland, American Society for Metals, Cleveland, pp. 3–31.